5 Quantum Bits and Quantum Gates

5.1 Single-qubit gates

5.1.1 Introduction

Information is quantized in classical digital information processing as well as in quantum information processing. In analogy to the classical bit, the elementary quantum of information in quantum information processing is called a *qubit*. Any two distinct states of a quantum system can be used as a qubit, as discussed in Chapter 4. The state of a qubit can be written as

$$|\Psi\rangle = a|0\rangle + b|1\rangle$$

with a, b complex and the normalization

$$|a|^2 + |b|^2 = 1.$$

Once some information is stored in a set of qubits (a quantum register), we must be able to manipulate these qubits in order to process the information. This means we must be able to change the state of a qubit either unconditionally (for example, for initializing a qubit or for writing information into a qubit), or conditionally, depending on the previous state of the qubit itself (e.g., the NOT operation) or on the state of itself and another qubit (e.g., the controlled NOT, or CNOT operation), and so on. These tasks have to be performed by *quantum gates*.

Like in the classical case, gate operations can in principle depend on the states of an arbitrary number of qubits. Fortunately all possible operations can be reduced to a finite set of *universal quantum gates*. From these gates one can construct the specific algorithms of quantum information processing which we discuss later.

In the present chapter we discuss the elementary building blocks for those algorithms: quantum gates. In several steps we show that arbitrary quantum gates can be constructed (or approximated to arbitrary precision) from a small number of one-and two-bit gates. Note that in Chapter 3 we argued that using *classical reversible* gates, three-bit operations are needed to achieve universality, whereas here we need only one- and two-qubit operations.

5.1.2 Example gates

All operators in the Hilbert space of a single qubit can be combined from the four fundamental operators $\mathbf{1}, \mathbf{X}, \mathbf{Y}$, and $\mathbf{Z}$ (the Pauli matrices), which form a complete and orthogonal basis for all possible operators. As an example, we consider the Hadamard gate $\mathbf{H}$, which can be written as the matrix representation

$$\mathbf{H}|\Psi\rangle = \frac{1}{\sqrt{2}} \begin{pmatrix} 1 & 1 \\ 1 & -1 \end{pmatrix} |\Psi\rangle$$

or as the rotation

$$\mathbf{H} = \frac{1}{\sqrt{2}}(\mathbf{X} + \mathbf{Z}),$$

as shown in (4.16). This corresponds to a π-rotation around the axis $\frac{1}{\sqrt{2}}(1, 0, 1)$.

Any unitary 2×2 matrix is a valid single-qubit quantum gate. Note that the operators $\mathbf{X}$, $\mathbf{Y}$, and $\mathbf{Z}$ have eigenvalues ± 1 and thus are unitary. It is evident why $\mathbf{X}$ is also often called the "NOT gate" in the language of quantum computing; $\mathbf{Z}$ generates a π relative phase between the two basis states, and $\mathbf{Y} = i\mathbf{XZ}$ is a combination of the two other gates.

To generate an arbitrary relative phase (instead of π) between the two states, we can use

$$e^{i\phi\mathbf{Z}} = \begin{pmatrix} e^{i\phi} & 0 \\ 0 & e^{-i\phi} \end{pmatrix}, \tag{5.1}$$

which generates a relative phase 2ϕ. If we apply this to a superposition state

$$|\Psi_0\rangle = \frac{1}{\sqrt{2}} \begin{pmatrix} 1 \\ 1 \end{pmatrix},$$

which is oriented at

$$\begin{pmatrix} \langle x \rangle \\ \langle y \rangle \\ \langle z \rangle \end{pmatrix} = \begin{pmatrix} 1 \\ 0 \\ 0 \end{pmatrix}.$$

we obtain

$$e^{i\phi \mathbf{Z}} |\Psi_0\rangle = \frac{1}{\sqrt{2}} \begin{pmatrix} e^{i\phi} \\ e^{-i\phi} \end{pmatrix}.$$

The corresponding vector rotates in the xy-plane:

$$\begin{pmatrix} \langle x \rangle \\ \langle y \rangle \\ \langle z \rangle \end{pmatrix} (\phi) = \begin{pmatrix} \cos 2\phi \\ \sin 2\phi \\ 0 \end{pmatrix}.$$

The rotation angle of the vector is therefore 2ϕ.

Important special cases of this gate are (up to an overall phase)

$$\begin{aligned} \mathbf{T} &= \begin{pmatrix} 1 & 0 \\ 0 & e^{i\pi/4} \end{pmatrix} \\ &= e^{i\pi/8} \begin{pmatrix} e^{-i\pi/8} & 0 \\ 0 & e^{i\pi/8} \end{pmatrix} \\ &= \exp(i\frac{\pi}{8}(1 - \mathbf{Z})) \end{aligned} \tag{5.2}$$

(the $\frac{\pi}{8}$ gate) and

$$\mathbf{S} = \mathbf{T}^2 = \begin{pmatrix} 1 & 0 \\ 0 & i \end{pmatrix}, \tag{5.3}$$

(often simply called the phase gate). Note that $\mathbf{S}^2 = \mathbf{Z}$.

The NOT gate can also be generalized. Due to the fact that $\mathbf{X}^2 = \mathbf{1}$ we have

$$\begin{aligned} \exp(i\phi\mathbf{X}) &= \mathbf{1}\cos\phi + i\mathbf{X}\sin\phi \\ &= \begin{pmatrix} \cos\phi & i\sin\phi \\ i\sin\phi & \cos\phi \end{pmatrix}, \end{aligned} \tag{5.4}$$

which interpolates smoothly between the identity and NOT gates, for $\phi = 0$ and $\frac{\pi}{2}$, respectively. For $\phi = \frac{\pi}{4}$ we obtain the "square-root of NOT" gate.

The gate $\exp(i\phi\mathbf{Y})$ may be discussed in a similar way.

5.1.3 General rotations

The above discussion of the spin component operators $\mathbf{X}, \mathbf{Y}$, and $\mathbf{Z}$ may be generalized to the spin operator component along an *arbitrary* direction. From the general theory of quantum mechanical angular momentum we know that $\exp(i\vec{q}\cdot\vec{\mathbf{S}})$ (for some vector $\vec{q}$) has the properties of a rotation operator. However, it is not always clear what is being rotated, and how. In Section 4.3.1 we studied the time evolution of the initial state $|\uparrow\rangle$ in a constant magnetic field $\vec{B}$ along one of the coordinate axes. The time evolution operator (4.17) in that case has precisely the form $\exp(i\vec{q}\cdot\vec{\mathbf{S}})$, with $\vec{q}$ along one of the axes. For $\vec{B}$ along the z axis we obtain no time evolution (apart from a trivial overall phase factor), but for $\vec{B}$ in the x direction, the state $|\psi(t)\rangle$ (4.20) is such that the expectation value of the spin vector $\vec{\mathbf{S}}$ rotates uniformly in the yz plane, that is, it rotates about the x axis. As the expectation value of the spin vector is proportional to the polarization vector $\vec{P}$ describing a state in the Bloch sphere representation (compare (4.32), (4.33)) we may also visualize $|\psi(t)\rangle$ as rotating on a circle on the surface of the Bloch sphere.

We now return to the case of a general rotation and consider the spin component operator $\vec{n}\cdot\vec{\mathbf{S}}$ along an arbitrary unit vector $\vec{n}$. Using the algebraic properties of the spin matrices, it is easy to show that the square of $\vec{n}\cdot\vec{\mathbf{S}}$ is a multiple of the unit operator,

$$\left(\frac{2}{\hbar}\vec{n}\cdot\vec{\mathbf{S}}\right)^2 = (n_x\mathbf{X} + n_y\mathbf{Y} + n_z\mathbf{Z})^2 = \mathbf{1},$$

and consequently the operator

$$\begin{aligned}\mathbf{R}_{\vec{n}}(\theta) &= \exp\left(i\theta\frac{2}{\hbar}\vec{n}\cdot\vec{\mathbf{S}}\right)\\ &= \mathbf{1}\cos\theta + i\frac{2}{\hbar}\vec{n}\cdot\vec{\mathbf{S}}\sin\theta\end{aligned}$$

generates a rotation around $\vec{n}$. For every rotation operator, we can get its inverse as

$$\mathbf{R}^{\dagger}_{\vec{n}}(\theta) = \mathbf{R}_{\vec{n}}(-\theta) = \mathbf{R}^{-1}_{\vec{n}}(\theta).$$

This operator obviously commutes with the spin component $\vec{n}\cdot\vec{\mathbf{S}}$ and thus does not affect this specific component. It can be shown that the unitary transformation $\mathbf{R}_{\vec{n}}(\theta)$ corresponds to a rotation by the angle 2θ about the axis $\vec{n}$, as shown in fig. 5.1. For $\vec{n} = (0,0,1)$ and $\theta = \pi/4$, the state is rotated as $(x \to -y \to -x \to y \to x)$. For other rotation axes, the sense of rotation is obtained from cyclic permutation $(x \to y \to z \to x)$.

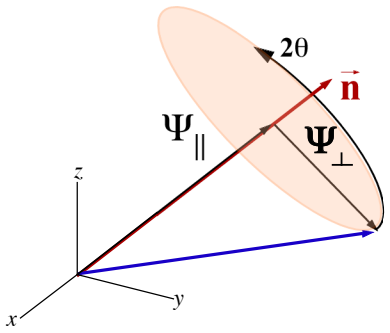

Figure 5.1: General rotation around an axis $\vec{n}$.

This rotation can be interpreted in several ways. The *expectation value* $\langle\vec{\mathbf{S}}\rangle$ of the spin vector rotates by 2θ as $\mathbf{R}_{\vec{n}}(\theta)$ is applied to the state of the qubit. Alternatively but equivalently we may think of the *spin vector* $\vec{\mathbf{S}}$ being rotated as it undergoes a unitary transformation, $\mathbf{R}^{\dagger}_{\vec{n}}(\theta)\vec{\mathbf{S}}\mathbf{R}_{\vec{n}}(\theta)$. Finally, the *polarization vector* $\vec{P}$ on the Bloch sphere rotates as $\langle\vec{\mathbf{S}}\rangle$ does.

We do not demonstrate explicitly that $\mathbf{R}_{\vec{n}}(\alpha)$ is a 2α rotation for general $\vec{n}$, but only for $\vec{n} = \hat{z}$ (the unit vector along the z axis):

$$\mathbf{R}_{\hat{z}}(\alpha) = \exp(i\alpha\mathbf{Z}) = \begin{pmatrix} e^{i\alpha} & 0\\ 0 & e^{-i\alpha}\end{pmatrix}.$$

For an arbitrary pure state $|\theta,\phi\rangle$ (compare (4.21)) we obtain

$$\begin{aligned}\mathbf{R}_{\hat{z}}(\alpha)|\theta,\phi\rangle &= \begin{pmatrix} e^{i\alpha} & 0\\ 0 & e^{-i\alpha}\end{pmatrix}\begin{pmatrix} e^{-i\frac{\phi}{2}}\cos\frac{\theta}{2}\\ e^{i\frac{\phi}{2}}\sin\frac{\theta}{2}\end{pmatrix}\\ &= \begin{pmatrix} e^{-i\frac{\phi-2\alpha}{2}}\cos\frac{\theta}{2}\\ e^{i\frac{\phi-2\alpha}{2}}\sin\frac{\theta}{2}\end{pmatrix}\\ &= |\theta,\phi-2\alpha\rangle.\end{aligned}$$

Since $\mathbf{R}_{\vec{n}}(\pi) = -\mathbf{1}$, every 2π rotation ($\alpha = \pi$) reverses the sign of any single-qubit state, but has no consequences for expectation values of physical observables in that state.

5.1.4 Composite rotations

As any normalized pure single-qubit state is represented by a point on the surface of the Bloch sphere, and as any two points on a sphere are connected by a rotation, any unitary single-qubit operator can be written in the form

$$\mathbf{U} = e^{i\alpha}\mathbf{R}_{\vec{n}}(\theta).$$

It is often desirable to employ only rotations about the coordinate axes instead of rotations about arbitrary axes $\vec{n}$. This is indeed possible; for any unitary $\mathbf{U}$ a decomposition

$$\mathbf{U} = e^{i\delta}\mathbf{R}_{\hat{z}}(\frac{\alpha}{2})\mathbf{R}_{\hat{y}}(\frac{\beta}{2})\mathbf{R}_{\hat{z}}(\frac{\gamma}{2}) \tag{5.5}$$

can be found.

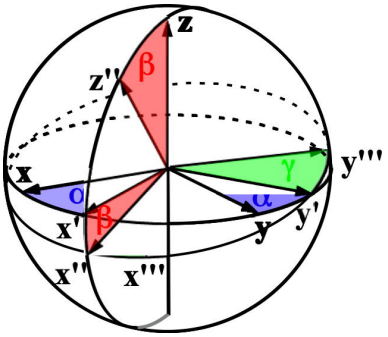

Figure 5.2: Decomposition of a rotation into Euler angles.

This procedure was introduced by Leonhard Euler (1707 - 1783) and the angles α, β, γ are therefore known as Euler angles. Figure 5.2 shows one of many possible combinations of rotation axes and angles, taking into account that the rotation generates by $\mathbf{R}_{\vec{n}}(\theta)$ is 2θ. Specifying the angles alone is not sufficient, but the corresponding axes must also be given. In addition, it is possible rotate the object or the coordinate axes.

As an example, we decompose the Hadamard gate $\mathbf{H}$ into

$$\mathbf{H} = \mathbf{R}_{\hat{y}}(\frac{\pi}{8})\mathbf{R}_{\hat{z}}(\frac{\pi}{2})\mathbf{R}_{\hat{y}}(-\frac{\pi}{8}).$$

Another decomposition which will be used in the next subsection is closely related to the above single-qubit $Z-Y$ decomposition. Let

$$\begin{aligned}\mathbf{A} &= \mathbf{R}_{\hat{z}}(\beta)\mathbf{R}_{\hat{y}}(\frac{\gamma}{2});\\ \mathbf{B} &= \mathbf{R}_{\hat{y}}(-\frac{\gamma}{2})\mathbf{R}_{\hat{z}}(-\frac{\delta+\beta}{2});\\ \mathbf{C} &= \mathbf{R}_{\hat{z}}(\frac{\delta-\beta}{2}),\end{aligned}$$

with β, γ, and δ determined from (5.5). Note that

$$\mathbf{ABC} = \mathbf{1}; \tag{5.6}$$

furthermore the relations between Pauli matrices

$$\mathbf{XYX} = -\mathbf{Y}; \quad \mathbf{XZX} = -\mathbf{Z}$$

can be used to show that

$$\mathbf{XBX} = \mathbf{R}_{\hat{y}}(\frac{\gamma}{2})\mathbf{R}_{\hat{z}}(\frac{\delta+\beta}{2})$$

and thus

$$\begin{aligned}\mathbf{AXBXC} &= \mathbf{R}_{\hat{z}}(\beta)\mathbf{R}_{\hat{y}}(\gamma)\mathbf{R}_{\hat{z}}(\delta) \qquad (5.7)\\ &= e^{-i\alpha}\mathbf{U} = \mathbf{R}_{\vec{n}}(\theta).\end{aligned}$$

The two $\mathbf{X}$ operators (NOT gates) have thus converted the unit operator (5.6) into the rotation operator $\mathbf{R}_{\vec{n}}(\theta)$.

5.2 Two-qubit gates

5.2.1 Controlled gates

Any programming language contains control structures of the type: "If condition X holds, perform operation Y". In quantum information processing these structures are implemented using multi-qubit gates which have one or more *control qubits* and *target qubits*. The simplest example is the two-bit (or two-qubit) operation known as "controlled NOT" (CNOT), defined by the truth table in Table 5.1.

control-qubit	target-qubit	result
0	0	00
0	1	01
1	0	11
1	1	10

Table 5.1: Truth table CNOT

The control qubit remains unchanged, but the target qubit is flipped if the control qubit is 1. (We abbreviate $|1\rangle$ as 1 here for simplicity.) The "result" column of the truth table lists both control and target qubits. The output target qubit is equal to that of the "exclusive or" (XOR) between the control and target qubits. Hence the CNOT operation is also called "reversible XOR", where the reversibility is accomplished by keeping the value of the control qubit, in contrast to the ordinary (irreversible) XOR operation of classical computer science which we discussed in Chapter 3. Like the single-qubit NOT, the reversible XOR is its own inverse. Symbolically it achieves the following mapping:

$$(x, y) \longrightarrow (x, x \text{ XOR } y), \tag{5.8}$$

and it can be used to copy a bit, because it maps

$$(x, 0) \longrightarrow (x, x).$$

Figure 5.3 shows how a combination of three CNOT gates (the second one with reversed roles of control and target bits) swaps the contents of

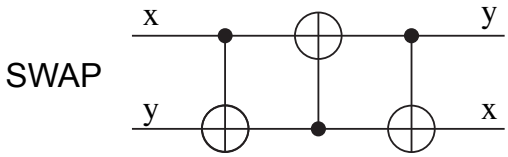

Figure 5.3: SWAP gate by combining 3 CNOT gates.

two bits ($x \leftrightarrow y$), as can be verified by repeated application of (5.8):

$$(x, y) \longrightarrow (y, x).$$

Thus the CNOT gate can be used to copy and move bits around.

In matrix notation with respect to the usual computational basis ($|00\rangle, |01\rangle, |10\rangle, |11\rangle$) the CNOT gate reads

$$\begin{aligned} \text{CNOT} &= \begin{pmatrix} 1 & 0 & 0 & 0 \\ 0 & 1 & 0 & 0 \\ 0 & 0 & 0 & 1 \\ 0 & 0 & 1 & 0 \end{pmatrix} \\ &= \begin{pmatrix} \mathbf{1} & \mathbf{0} \\ \mathbf{0} & \mathbf{X} \end{pmatrix} \end{aligned}$$

(using 2×2 block matrix notation). Replacing $\mathbf{X}$ by an arbitrary unitary single-qubit operation $\mathbf{U}$, we arrive at the *controlled-U* (CU) gate.

5.2.2 Composite gates

The roles of control and target qubits may be shifted by basis transformations (in the individual qubit Hilbert spaces). One example is shown in figure 5.4.

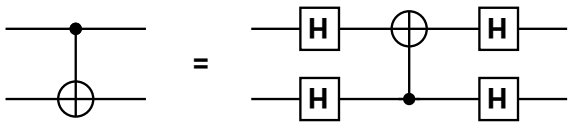

Figure 5.4: Ambiguity of control and target qubits.

Here control and target qubits have interchanged their roles due to the application of a Hadamard gate (4.16) to each qubit both before and after the CNOT operation. This can be verified by writing down the two-qubit Hadamard transform matrix $\mathbf{H}_1 \otimes \mathbf{H}_2$ explicitly and performing the matrix multiplications.

The CU gate can be implemented using CNOT and single-qubit gates. The idea is to use the decomposition (5.7) and apply $\mathbf{U} = e^{i\alpha}\mathbf{AXBXC}$ if the control qubit is set and $\mathbf{ABC} = \mathbf{1}$ if not. The circuit in Figure 5.5 does the trick. Obviously the $e^{i\alpha}$ phase factor as well as the two NOT ($= \mathbf{X}$) operations are only active if the control qubit is set.

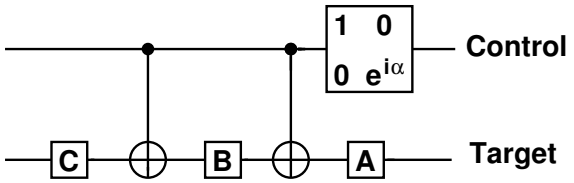

Figure 5.5: A circuit for the controlled-U gate.

The CNOT and Hadamard gates can be used, for example, to create maximally entangled states from the four two-qubit computational basis states $|a, b\rangle$ (with $a, b = 0, 1$) via

$$|\beta_{ab}\rangle = \text{CNOT}\ (a, b)\mathbf{H}(a)|a, b\rangle$$

As an example, consider

$$\begin{aligned} \mathbf{H}(a)|0, 0\rangle &= \frac{1}{\sqrt{2}}(|0, 0\rangle + |1, 0\rangle) \\ \Rightarrow\ |\beta_{00}\rangle &= \frac{1}{\sqrt{2}}(|0, 0\rangle + |1, 1\rangle). \end{aligned}$$

which is one of the Bell states (4.28). The other (a,b) values yield the remaining members of the Bell basis.

If a Hadamard gate is applied to each qubit of the ground state $|0, 0, \ldots 0\rangle$, the resulting state (here, as an example, for 2 qubits,) is

$$\begin{aligned} \mathbf{H}\,|0, 0\rangle &= \frac{1}{2}(|0\rangle + |1\rangle) \otimes (|0\rangle + |1\rangle) \\ &= \frac{1}{2}(|00\rangle + |01\rangle + |10\rangle + |11\rangle). \end{aligned}$$

The other computational basis states are transformed into

$$\begin{pmatrix} |00\rangle \\ |01\rangle \\ |10\rangle \\ |11\rangle \end{pmatrix} \overset{H}{\Rightarrow} \frac{1}{2} \begin{pmatrix} |00\rangle + |01\rangle + |10\rangle + |11\rangle \\ |00\rangle - |01\rangle + |10\rangle - |11\rangle \\ |00\rangle + |01\rangle - |10\rangle - |11\rangle \\ |00\rangle - |01\rangle - |10\rangle + |11\rangle \end{pmatrix}.$$

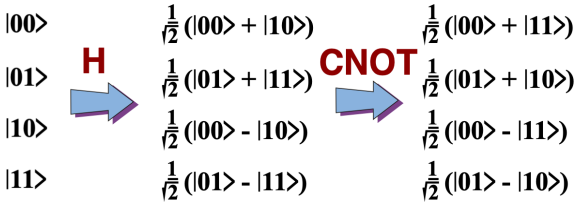

Figure 5.6: Generating the Bell states from the computational basis states.

As shown in Figure 5.6, these states can be converted into the Bell states by applying a CNOT operation to them.

5.2.3 3-qubit gates

In higher-order controlled operations n control qubits and k target qubits are used; an important example is the Toffoli (controlled-controlled-NOT, or C^{2}NOT) gate (3.4), or more generally, the C^{2}U gate for some arbitrary single-qubit $\mathbf{U}$. C^{2}U can be built from CNOT and single-qubit gates. To see this, consider the unitary operator $\mathbf{V}$, with $\mathbf{V}^2 = \mathbf{U}$ (which always exists) and build the circuit shown in Figure 5.7.

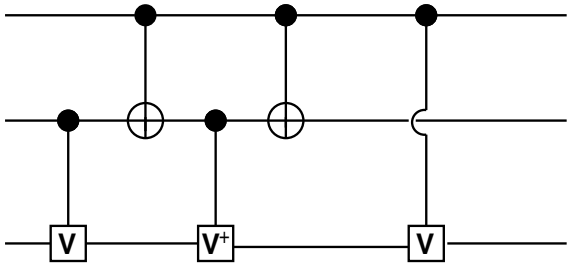

Figure 5.7: A circuit for the controlled-controlled-U gate; $\mathbf{V}^2 = \mathbf{U}$.

If neither of the control qubits is set, nothing at all happens. If only one control qubit is set, $\mathbf{V}^\dagger = \mathbf{V}^{-1}$ and one $\mathbf{V}$ acts on the target qubit. If both control qubits are set, $\mathbf{V}^\dagger$ is not switched on, but both $\mathbf{V}$s are.

This is an example how 3-qubit quantum gates like the Toffoli gate can be decomposed into one- and two-qubit gates, which is not possible classically. (Otherwise universal reversible classical computation with just one- and two-bit operations would be possible, contrary to what we discussed in Chapter 3.) The Toffoli gate (and as we shall see, *any* gate) can be made from Hadamard (more precisely, square root of Hadamard), phase, CNOT, and $\frac{\pi}{8}$ gates.

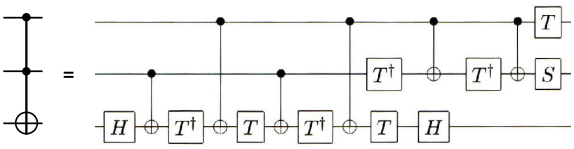

Figure 5.8: Decomposition of the Toffoli gate into 1- and 2-qubit gates.

Figure 5.8 shows how the Toffoli gate can be decomposed into about a dozen more elementary gates. Here,

$$T = \begin{pmatrix} 1 & 0 \\ 0 & e^{i\pi/4} \end{pmatrix} = e^{i\pi/8} e^{-i\pi/8\,\mathbf{Z}}$$

is the $\pi/8$ gate and $\mathbf{S} = \mathbf{T^2}$ is called the phase gate.

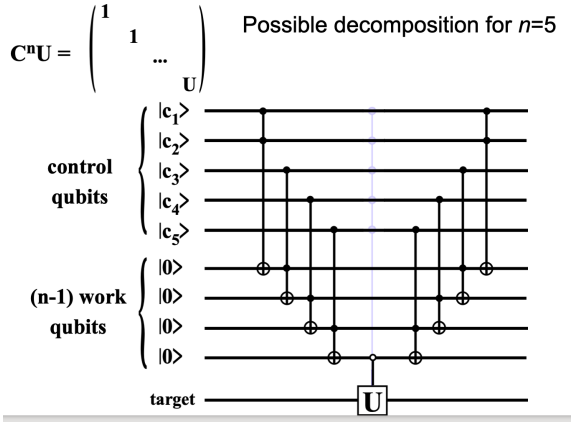

Figure 5.9: Decomposition of a $\mathbf{C^nU}$ into Toffoli and $\mathbf{U}$ gates.

Figure 5.9 shows, as another example of a decomposition, how a $\mathbf{C^nU}$ gate can be built from Toffoli and $\mathbf{U}$ gates, for the case of $n = 5$. $\mathbf{U}$ is a 2×2 unitary gate that is only active if all control qubits are 1.

5.3 Universal sets of gates

5.3.1 Choice of set

It is important to know whether any conceivable unitary operation in the Hilbert space of interest can be decomposed into a sequence of standard elementary operations taken from a finite set. Only if that is true, can a universal quantum computer be built which can be programmed to fulfill fairly arbitrary tasks, much as today's universal classical digital computers which are (in principle) built from a very small set of universal classical gates. Luckily there exists a set of *universal quantum gates*, in the sense that any unitary operation may be *approximated* to arbitrary accuracy by a combination of these gates.

As already mentioned in the previous section, the following four gates do the trick:

- the CNOT gate,
- the $\frac{\pi}{8}$ gate (5.2)

$$\mathbf{T} = \begin{pmatrix} 1 & 0 \\ 0 & \exp i\frac{\pi}{4} \end{pmatrix} = \exp\left(i\frac{\pi}{8}(\mathbf{1} - \mathbf{Z})\right),$$

- the phase gate (5.3)

$$\mathbf{S} = \mathbf{T}^2 = \begin{pmatrix} 1 & 0 \\ 0 & i \end{pmatrix}$$

  (note that $\mathbf{S}^2 = \mathbf{Z}$), and
- the square root $\mathbf{H}^{\frac{1}{2}}$ of the Hadamard gate[1] (4.16)

$$\mathbf{H}^{\frac{1}{2}} = \frac{e^{\mp i\frac{\pi}{4}}}{\sqrt{2}}(\mathbf{1} \pm i\mathbf{H}) = \mathbf{H}^{-\frac{1}{2}} \qquad (5.9)$$

[1] Since $\mathbf{H}$ is its own inverse, the square roots of $\mathbf{H}$ and $\mathbf{H}^{-1}$ are equal. Consequently $\mathbf{H}^{\frac{1}{2}}$ and $\mathbf{H}^{-\frac{1}{2}}$ are not inverses to each other; however, $\mathbf{H}_+^{\frac{1}{2}}\mathbf{H}_-^{-\frac{1}{2}} = \mathbf{1}$, where the subscript denotes the two possibilities in (5.9)

This set of four gates can be shown to be universal in a three-step process.

1. Any unitary operator can be expressed (exactly) as a product of unitary operators affecting only two computational basis states: "Two-level gates are universal."
2. (From 1) and preceding sections.) Any unitary operator may be expressed (exactly) using single-qubit and CNOT gates: "Single-qubit and CNOT gates are universal."
3. Single-qubit operations may be *approximated* to arbitrary accuracy using square root of Hadamard, phase, and $\frac{\pi}{8}$ gates.

5.3.2 Unitary operations

We start with step 1: Two-level gates are universal; that is, any $d \times d$ unitary matrix $\mathbf{U}$ can be written as a product of (at most) $\frac{d(d-1)}{2}$ two-level unitary matrices (unitary matrices that act non-trivially only on at most two vector components). This can be shown as follows. Concentrate on the top left corner of the unitary matrix

$$\mathbf{U} = \begin{pmatrix} a & d & \cdots \\ b & c & \cdots \\ \cdot & \cdot & \cdots \end{pmatrix}.$$

The 2×2 unitary matrix

$$\mathbf{U}_1 = \frac{1}{\sqrt{|a|^2 + |b|^2}} \begin{pmatrix} a^* & b^* \\ b & -a \end{pmatrix}$$

eliminates the second element in the first column of $\mathbf{U}$:

$$\mathbf{U}_1 \begin{pmatrix} a \\ b \end{pmatrix} = \begin{pmatrix} a' \\ 0 \end{pmatrix}.$$

(In what follows we use (without introducing additional notation) $\mathbf{U}_1$, supplemented by a $(d-2) \times (d-2)$ unit matrix so that products like $\mathbf{U}_1\mathbf{U}$ make sense.) Further unitary 2×2 matrices can be used to eliminate further elements

from the first column of $\mathbf{U}$:

$$\mathbf{U}_{d-1}\mathbf{U}_{d-2}\cdots\mathbf{U}_1\mathbf{U} = \begin{pmatrix} 1 & 0 & 0 & \cdots \\ 0 & c' & \cdot & \cdots \\ 0 & \cdot & \cdot & (\text{non-zero}) \\ \cdot & & & \end{pmatrix} .$$

Note that initially the first column had unit norm because $\mathbf{U}$ is unitary. We have applied only unitary (that is, norm-preserving) operations so the end result is still a unit vector but has only one non-zero component, which must be 1. (A phase can be eliminated.) Due to unitarity (of a product of unitary matrices) all elements in the first row other than the leftmost one must also vanish. The elimination process can be continued in other columns and finally

$$\mathbf{U}_k\mathbf{U}_{k-1}\cdots\mathbf{U}_1\mathbf{U} = \mathbf{1}$$
$$\left(k \le \frac{d(d-1)}{2} = (d-1) + (d-2) + \cdots + 1\right)$$

$$\mathbf{U}_k\mathbf{U}_{k-1}\cdots\mathbf{U}_1\mathbf{U} = \mathbf{1}$$
$$\left(k \le \frac{d(d-1)}{2} = (d-1) + (d-2) + \cdots + 1\right)$$

and thus

$$\mathbf{U} = \mathbf{U}_1^\dagger\mathbf{U}_2^\dagger\cdots\mathbf{U}_k^\dagger$$

which is the desired decomposition of an arbitrary gate $\mathbf{U}$ in terms of two-level gates.

5.3.3 Two qubit operations

In step 2 we prove that single-qubit and CNOT gates are universal, because we can use them to build the arbitrary two-level gates discussed in the previous step. The basic idea is simple. Transform the Hilbert space such that the two relevant basis states become the basis states of one qubit, perform the desired single-qubit operation on that qubit, and transform back to the original basis. The basis reshuffling can be achieved via higher-order controlled-NOT operations, which in turn can be reduced to simple CNOT operations.

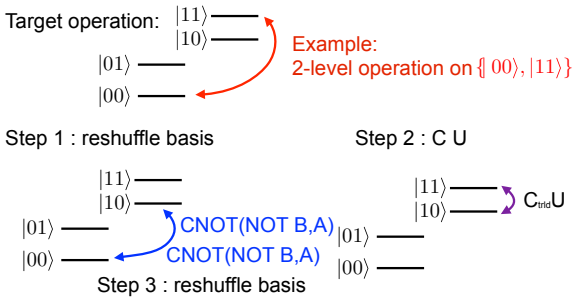

Figure 5.10: Example of a decomposition of a 2-level operation on 2 qubits into CNOT and a single-qubit operations.

Figure 7.26 shows the scheme for a 2-qubit system: to apply a 2-level operation between $|00\rangle$ and $|11\rangle$, we first swap the states $|00\rangle \leftrightarrow |10\rangle$ with a CNOT gate. Then the **CU**operation can be applied and finally the basis is brought back to the original state.

For a three-qubit example, we discuss how to perform a two-level operation $\mathbf{U}$ on the states $|ABC\rangle = |000\rangle$ and $|111\rangle$. First, apply the Toffoli gate $\theta^{(3)}$ (3.4) to the three arguments NOT A, NOT B, and C(remember that the Toffoli gate is a three-qubit gate): $\theta^{(3)}(\text{ NOT } A, \text{ NOT } B, C)$. The first two qubits are control qubits which in this case must be 0, the last one is the target. This operation swaps $|000\rangle$ with $|001\rangle$ and leaves everything else untouched. Now, apply $\theta^{(3)}(\text{ NOT } A, C, B)$. This swaps $|001\rangle$ with $|011\rangle$. The net effect has been to swap $|000\rangle$ with $|011\rangle$. Now, the $\mathrm{C}^2\mathrm{U}$ can be applied, performing the operation $\mathbf{U}$ on qubit A, provided both B and C are 1. Finally the basis states can be rearranged in their original order.

Similar rearrangements can always be achieved through a sequence of qubit basis states (or the binary numbers representing the states) two consecutive members of which differ at one position only. (Such sequences are known as *Gray codes*.) Clearly this way of constructing arbitrary quantum gates is not always the most efficient one (involving the smallest possible number of operations). However, this is no source of serious

concern, since there are, in any case, unitary n-qubit operations which involve $O(e^n)$ gates to implement (see Section 4.5.4 of [35]) and hence are intrinsically inefficient.

5.3.4 Approximating single-qubit gates

In step 3 we show that Hadamard, phase and $\pi/8$ gates are (approximately) universal single-qubit gates. Recall that the most general single-qubit gate is a rotation by an arbitrary angle about an arbitrary axis (combined with a trivial phase factor). Imagine we could implement a rotation about some axis $\vec{n}$ by an angle α which is an *irrational* multiple of 2π. Due to irrationality, the angles

$$n\alpha \mod 2\pi \quad (n = 0, 1, 2, ...)$$

are dense in $[0, 2\pi]$ and thus an arbitrary rotation about $\vec{n}$ can be approximated to arbitrary precision by repeating the α rotation:

$$\mathbf{R}_{\vec{n}}(\beta) = (\mathbf{R}_{\vec{n}}(\alpha))^{\nu} + O(\epsilon).$$

If we can implement two such irrational rotations about mutually orthogonal axes we can perform arbitrary rotations due to the Z-Y-Z decomposition (5.5). This is exactly the route followed by Boykin *et al.* [66] which we will briefly sketch now. From the fundamental multiplication laws for Pauli matrices

$$\mathbf{X}^2 = \mathbf{Y}^2 = \mathbf{Z}^2 = \mathbf{1}, \quad \mathbf{XY} = i\mathbf{Z} = -\mathbf{YX} \quad \text{etc.}$$

and the definition of the Hadamard gate

$$\mathbf{H} = \frac{1}{\sqrt{2}}(\mathbf{X} + \mathbf{Z}),$$

we obtain

$$\mathbf{HXH} = \mathbf{Z}, \quad \mathbf{HZH} = \mathbf{X}.$$

Furthermore we recall the rotation of the Bloch sphere about the unit vector $\vec{n}$ by an angle θ

$$\exp\left(-i\frac{\theta}{2}\vec{n}\cdot\vec{\sigma}\right) = \cos\left(\frac{\theta}{2}\right)\mathbf{1} - i\sin\left(\frac{\theta}{2}\right)\vec{n}\cdot\vec{\sigma},$$

($\vec{\sigma} = (\mathbf{X}, \mathbf{Y}, \mathbf{Z}) = \frac{2}{\hbar}\vec{\mathbf{S}}$), and the $\frac{\pi}{8}$ gate

$$\begin{aligned}\mathbf{T} &= e^{i\frac{\pi}{8}}\begin{pmatrix} e^{-i\frac{\pi}{8}} & 0 \\ 0 & e^{i\frac{\pi}{8}} \end{pmatrix} = e^{i\frac{\pi}{8}}e^{-i\frac{\pi}{8}\mathbf{Z}} = \mathbf{Z}^{\frac{1}{4}} \\ &\Rightarrow \quad \mathbf{HTH} = e^{i\frac{\pi}{8}}e^{-i\frac{\pi}{8}\mathbf{X}} = \mathbf{X}^{\frac{1}{4}}.\end{aligned}$$

We now multiply

$$\begin{aligned}& \mathbf{Z}^{-\frac{1}{4}}\mathbf{X}^{\frac{1}{4}} \\ =\ & e^{i\frac{\pi}{8}\mathbf{Z}}e^{-i\frac{\pi}{8}\mathbf{X}} \\ =\ & \left(\cos\left(\frac{\pi}{8}\right)\mathbf{1} + i\sin\left(\frac{\pi}{8}\right)\mathbf{Z}\right) \\ & \cdot\left(\cos\left(\frac{\pi}{8}\right)\mathbf{1} - i\sin\left(\frac{\pi}{8}\right)\mathbf{X}\right) \\ =\ & \cos^2\left(\frac{\pi}{8}\right)\mathbf{1} - i\sin\left(\frac{\pi}{8}\right) \\ & \cdot\left(\cos\left(\frac{\pi}{8}\right)\mathbf{X} - \sin\left(\frac{\pi}{8}\right)\mathbf{Y} - \cos\left(\frac{\pi}{8}\right)\mathbf{Z}\right) \\ =\ & \cos^2\left(\frac{\pi}{8}\right)\mathbf{1} - i\sin\left(\frac{\pi}{8}\right)\vec{q}\cdot\vec{\sigma},\end{aligned}$$

where

$$\vec{q} = \begin{pmatrix} \cos\left(\frac{\pi}{8}\right) \\ -\sin\left(\frac{\pi}{8}\right) \\ -\cos\left(\frac{\pi}{8}\right) \end{pmatrix}.$$

With $\vec{n} = \frac{\vec{q}}{|\vec{q}|}$ this can be written as

$$\mathbf{Z}^{-\frac{1}{4}}\mathbf{X}^{\frac{1}{4}} = \cos\alpha\mathbf{1} - i\sin\alpha\,\vec{n}\cdot\vec{\sigma}$$

where

$$\cos\alpha = \cos^2\left(\frac{\pi}{8}\right) = \frac{1}{2}\left(1 + \frac{1}{\sqrt{2}}\right).$$

Invoking some theorems from algebra and number theory it can be shown that α is an irrational multiple of 2π.

This is the first of the two rotations we need. The second one is

$$\mathbf{H}^{-\frac{1}{2}}\mathbf{Z}^{-\frac{1}{4}}\mathbf{X}^{\frac{1}{4}}\mathbf{H}^{\frac{1}{2}},$$

where

$$\mathbf{H}^{-\frac{1}{2}} = \frac{e^{-i\frac{\pi}{4}}}{\sqrt{2}}(\mathbf{1} + i\mathbf{H}). \tag{5.10}$$

Now we can work out

$$\begin{aligned}\mathbf{H}^{-\frac{1}{2}}\mathbf{X}\mathbf{H}^{\frac{1}{2}} &= \frac{1}{2}(\mathbf{X}+\mathbf{Z}-\sqrt{2}\mathbf{Y})\\ \mathbf{H}^{-\frac{1}{2}}\mathbf{Y}\mathbf{H}^{\frac{1}{2}} &= \frac{1}{\sqrt{2}}(\mathbf{X}-\mathbf{Z})\\ \mathbf{H}^{-\frac{1}{2}}\mathbf{Z}\mathbf{H}^{\frac{1}{2}} &= \frac{1}{2}(\mathbf{X}+\mathbf{Z}+\sqrt{2}\mathbf{Y}),\end{aligned}$$

and finally

$$\mathbf{H}^{-\frac{1}{2}}\mathbf{Z}^{-\frac{1}{4}}\mathbf{X}^{\frac{1}{4}}\mathbf{H}^{\frac{1}{2}} = \cos^2\left(\frac{\pi}{8}\right)\mathbf{1} - i\sin\left(\frac{\pi}{8}\right)\vec{m}\cdot\vec{\sigma}$$

with

$$\vec{m} = \begin{pmatrix} -\frac{1}{\sqrt{2}}\sin\left(\frac{\pi}{8}\right) \\ -\sqrt{2}\cos\left(\frac{\pi}{8}\right) \\ \frac{1}{\sqrt{2}}\sin\left(\frac{\pi}{8}\right)\end{pmatrix}$$

from which we see that $\vec{m}^2 = \vec{q}^2$ and $\vec{m}\cdot\vec{q} = 0$. This is again a rotation by the same angle α as before, about an axis orthogonal to the previous axis $\vec{n}$.

The construction in [35] uses the rotations $\mathbf{X}^{\frac{1}{4}}\mathbf{Z}^{\frac{1}{4}}$ and $\mathbf{H}\mathbf{X}^{\frac{1}{4}}\mathbf{Z}^{\frac{1}{4}}\mathbf{H} = \mathbf{Z}^{\frac{1}{4}}\mathbf{X}^{\frac{1}{4}}$, which are quite similar to those used above. However, the axes of rotation are not orthogonal to each other but only at an angle of 32.65°. In this case the simple Z-Y-Z decomposition (5.5) of an arbitrary rotation into three factors is not possible, but a decomposition into more than three factors still is.

5.4 Resonant electromagnetic fields

So far we assumed that the gate operation is driven by a (magnetic) field, which causes Larmor precession of the pseudo-spin. In practice, it is more common and more effective to use time-dependent electromagnetic fields whose frequency is close to the transition frequency between two stationary states.

5.4.1 Radio frequency field

To excite transitions between the different spin states and implement quantum gate operations, one applies a ardio-frequency (RF) magnetic field. It is generated by a current running through a coil that is wound around the sample, as shown in Figure 5.11.

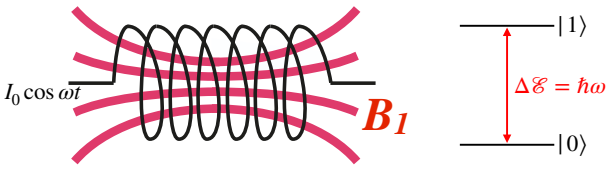

Figure 5.11: An alternating current through a coil generates an RF field resonant with the transition between 2 qubit states.

The generated RF field is

$$\vec{B}_{rf}(t) = 2B_1\cos(\omega t)\begin{pmatrix}1\\0\\0\end{pmatrix},$$

where we have chosen the x-axis along the axis of the coil. In this case, the ac field couples to the S_x component of the spin.

This linearly oscillating magnetic field is best described as a superposition of two fields rotating in opposite directions.

$$\vec{B}_{rf}(t) = B_1\begin{pmatrix}\cos(\omega t)\\ \sin(\omega t)\\ 0\end{pmatrix} + B_1\begin{pmatrix}\cos(\omega t)\\ -\sin(\omega t)\\ 0\end{pmatrix}.$$

The first component rotates from x to the y axis (counterclockwise when viewed from the z-axis), the second in the opposite direction.

If we combine this alternating field with the static Hamiltonian (for the spin case, e.g. a Zeeman field along z) into a time-dependent Hamiltonian, we obtain an equation of motion with time-dependent coefficients, which cannot be solved analytically. This holds true for all qubit systems that are excited by resonantly oscillating control fields. This problem can be

solved by moving the time-dependence from the control fields to the coordinate system. For reasons that will become clear, the associated reference frame is known as the rotating frame.

5.4.2 Rotating frame

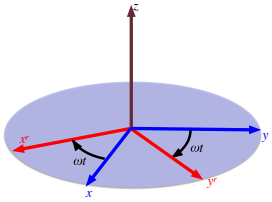

Figure 5.12: Rotating and laboratory-fixed coordinate systems.

The resulting dynamics are best analyzed in a coordinate system that rotates around the static magnetic field at the RF frequency. We briefly show here the transformation to this rotating frame since all quantum computing experiments use the rotating frame representation, not the laboratory frame. As shown in Figure 5.12, the two coordinate systems are related by

$$\begin{pmatrix} x \\ y \\ z \end{pmatrix}^r = \begin{pmatrix} \cos(\omega t) & \sin(\omega t) & 0 \\ -\sin(\omega t) & \cos(\omega t) & 0 \\ 0 & 0 & 1 \end{pmatrix} \begin{pmatrix} x \\ y \\ z \end{pmatrix}.$$

where the vector $\vec{r}^r$ refers to the rotating coordinate system, the unlabeled one to the laboratory-fixed system.

If we apply this transformation to the RF field, the two circular components become

$$\vec{B}^r_{rf} = +B_1 \begin{pmatrix} 1 \\ 0 \\ 0 \end{pmatrix} + B_1 \begin{pmatrix} \cos(2\omega t) \\ -\sin(2\omega t) \\ 0 \end{pmatrix}.$$

Figure 5.13 shows a graphic representation of this transformation.

Apparently, one of the two components is now static, while the counter-rotating component rotates at twice the RF frequency. It turns out that, to an excellent approximation, it is sufficient to consider the effect of that component

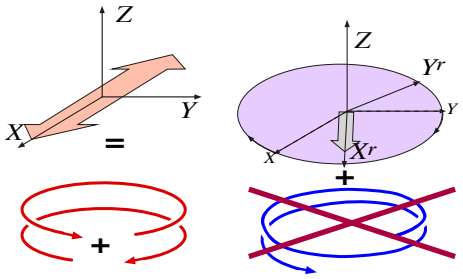

Figure 5.13: Circularly polarized components of the linearly polarized field in laboratory frame (left) and rotating frame (right).

which is static in this coordinate system, while the counter-rotating component can be neglected [67]. It is therefore a convenient fiction to assume that the applied RF generates a circularly polarized RF field, which is static in the rotating frame. The corresponding Hamiltonian is

$$\mathcal{H}^r_{rf} = -\omega_1 \mathbf{S}_x. \tag{5.11}$$

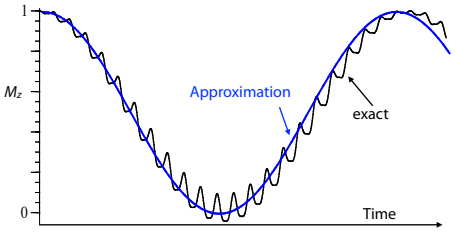

Figure 5.14: Comparison between the exact solution and the rotating wave approximation.

Under most conditions, this approximation yields an excellent description of the actual dynamics. Figure 5.14 compares the exact evolution to the result of the rotating wave approximation. Compared to typical experimental situations, for this figure the parameters have been chosen to exaggerate the deviations by several orders of magnitude. The rapid oscillation occurs at twice the Larmor frequency. In addition, the frequency is shifted slightly, by $\frac{1}{4}\frac{\omega_1^2}{\omega_L}$.

The same reasoning can be used in any type of resonant excitation. In the case of optical spec-

troscopy (e.g. trapped ion quantum computers), it is known as the rotating wave approximation.

5.4.3 Equation of motion

So far we have transformed the RF field into the rotating frame. We also need to transform the quantum mechanical equation of motion into this reference frame. We write the static Hamiltonian as

$$\mathcal{H}_z = -\gamma\,\mathbf{S}_z B_0 = -\omega_L \mathbf{S}_z \tag{5.12}$$

and start by transforming the state vector, using the unitary operator

$$\mathbf{U}(t) = e^{i\omega t \mathbf{S}_z/\hbar}, \tag{5.13}$$

which defines a rotation around the z-axis and commutes with the static Hamiltonian. It transforms the laboratory state $|\psi\rangle$ into the rotating frame as

$$|\psi\rangle^r = \mathbf{U}^{-1}|\psi\rangle = e^{-i\omega t \mathbf{S}_z/\hbar}|\psi\rangle. \tag{5.14}$$

To transform an operator A into the same basis, we use

$$A^r = \mathbf{U^{-1}} A\,\mathbf{U}. \tag{5.15}$$

This is valid for all operators, including the density operator or the observables $\mathbf{S}_x$, $\mathbf{S}_y$ and $\mathbf{S}_z$. The only exception that needs special attention is the Hamiltonian.

In the case of the Hamiltonian, the transformation has to fulfill the additional requirement that the Hamiltonian remains the generator of the time evolution. Since the transformation $\mathbf{U}$ is time-dependent, the new coordinate system is not an inertial frame of reference. The evolution in this system therefore appears to be subject to additional 'virtual forces' that influence the time evolution and must be accounted for by the transformation. This is in close analogy to centrifugal forces or Coriolis forces that appear if the coordinate system rotates with respect to inertial frames of reference.

Starting with the Schrödinger equation in the laboratory frame

$$\hbar\frac{d}{dt}|\Psi\rangle(t) = -i\mathcal{H}|\Psi\rangle(t),$$

we use eq. (5.14) to substitute

$$|\Psi\rangle(t) = \mathbf{U}|\Psi\rangle^r(t)$$

and obtain an equation of motion for $|\Psi\rangle^r(t)$:

$$\hbar\frac{d}{dt}\left(\mathbf{U}|\Psi\rangle^r(t)\right) = -i\mathcal{H}\mathbf{U}|\Psi\rangle^r(t). \tag{5.16}$$

The left-hand side can be evaluated with the product-rule:

$$\frac{d}{dt}\left(\mathbf{U}|\Psi\rangle^r(t)\right) = \dot{\mathbf{U}}|\Psi\rangle^r(t) + \mathbf{U}\frac{d}{dt}|\Psi\rangle^r(t)$$

Inserting this into eq. (5.16), rearranging and multiplying with $\mathbf{U}^{-1}$ from the left yields

$$\hbar\frac{d}{dt}|\Psi\rangle^r(t) = -i\mathbf{U}^{-1}\mathcal{H}\mathbf{U}|\Psi\rangle^r(t) - \hbar\mathbf{U}^{-1}\dot{\mathbf{U}}|\Psi\rangle^r(t).$$

The Schrödinger equation in the rotating frame becomes therefore

$$\hbar\frac{d}{dt}|\Psi\rangle^r(t) = -i\mathcal{H}^r|\Psi\rangle^r(t)$$

with the transformed Hamiltonian

$$\mathcal{H}^r = \mathbf{U}^{-1}\mathcal{H}\mathbf{U} - i\hbar\mathbf{U}^{-1}\dot{\mathbf{U}} \tag{5.17}$$

The first term corresponds to the rotation (5.15) of the operator around the z-axis, as for the other operators. The second term takes into account that the rotating coordinate system is not an inertial reference frame, since the rotation is an accelerated motion. Like centrifugal forces, it corrects the equation of motion for the corresponding virtual force. Evaluating this term for the transformation operator 5.13, we find

$$\begin{aligned}\dot{\mathbf{U}} &= \frac{d}{dt}\left(e^{i\omega t\mathbf{S}_z/\hbar}\right)\\ &= \frac{i\omega}{\hbar}\mathbf{S}_z\mathbf{U}\\ -i\hbar\mathbf{U}^{-1}\dot{\mathbf{U}} &= -i\hbar\cdot\frac{i\omega}{\hbar}\mathbf{S}_z = \omega\mathbf{S}_z.\end{aligned}$$

This represents an additional term to the static Hamiltonian, modifying the level splitting. Combining it with the driving Hamiltonian (5.11), we obtain the rotating frame Hamiltonian

$$\begin{aligned}\mathcal{H}^r &= -(\omega_L - \omega)\mathbf{S}_z - \omega_1 \mathbf{S}_x \\ &= -\Delta\omega_L \mathbf{S}_z - \omega_1 \mathbf{S}_x \\ &= -\vec{\omega}_{\text{eff}} \cdot \vec{\mathbf{S}},\end{aligned}$$

where

$$\vec{\omega}_{\text{eff}} = \begin{pmatrix} \omega_1 \\ 0 \\ \Delta\omega_L \end{pmatrix}$$

is the total effective field in the rotating frame, $\omega_1 = \gamma B_1$ is the strength of the RF field in (angular) frequency units and $\Delta\omega_L = \omega_L - \omega$ is the static magnetic field (also in frequency units), reduced by the frequency of the applied field.

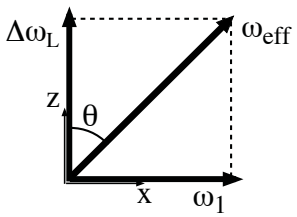

Figure 5.15: Effective magnetic field in the rotating coordinate system.

Figure 5.15 shows this vector graphically. The angle θ between $\vec{\omega}_{\text{eff}}$ and the z-axis is given by

$$\tan\theta = \frac{\omega_1}{\Delta\omega_L}.$$

5.4.4 Evolution

In the rotating frame, the effective Hamiltonian is time-independent (after neglecting the counterrotating term). It is therefore possible to describe the resulting evolution analytically: The evolution of the spins in the rotating frame is exactly the same as if a (small) static field were applied in this direction in the laboratory frame: they undergo a precession around the magnetic field $\vec{\omega}_{eff}$.

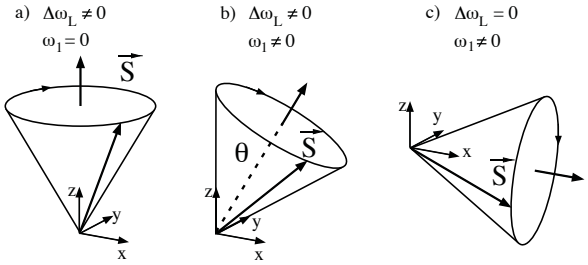

Figure 5.16: Spin precession for the cases of free precession ($\omega_1 = 0$, left), resonant irradiation ($\Delta\omega_L = 0$, right), and the general case (center).

Figure 5.16 shows three specific examples for the motion of spins in this effective field. In the absence of RF irradiation ($\omega_1 = 0$), the effective field is aligned with the z-axis and the precession is the same as in the laboratory frame, except that the precession frequency is reduced by ω, the frequency of the applied RF field. In the case of resonant irradiation (shown on the right), the field along the z-axis vanishes and the effective field lies along the x-axis. In the general case b), the effective field lies along a direction in the xz plane.

So far, we have assumed that the direction of the RF field coincides with the x-axis in the rotating frame. This can be changed by shifting the phase of the applied rf signal. As a function of this phase φ, the coupling Hamiltonian in the rotating frame becomes

$$\mathcal{H}^r_{rf} = -\omega_1(\cos\varphi\,\mathbf{S}_x + \sin\varphi\,\mathbf{S}_y)$$

and the effective field

$$\vec{\omega}_{\text{eff}} = \begin{pmatrix} \omega_1\cos\varphi \\ \omega_1\sin\varphi \\ \Delta\omega_L \end{pmatrix}. \tag{5.18}$$

As a simple example, we consider the case that the RF is applied on resonance, with $\varphi = 0$, such that $\vec{\omega}_{\text{eff}} = (\omega_1, 0, 0)$. If the spin is initially aligned with the z-axis, it rotates around the x-axis as

$$\rho(t) = \mathbf{S}_z\cos(\omega_1 t) + \mathbf{S}_y\sin(\omega_1 t). \tag{5.19}$$

The spin thus rotates from the z- to the y-axis and from there to the negative z-axis. Such a rotation by an angle $\omega_1 \tau_p = \pi$, with τ_p the duration of the pulse, corresponds to an inversion of the spins. If the field is left on, the spins continue to precess, returning to the $+z$ axis, again to the negative and so on. This process of successive inversions is called Rabi flopping, in reference to Rabi's molecular beam experiment [68]. The frequency ω_1 at which this process occurs is called the Rabi frequency.

The primary use of irradiation with ac fields in quantum computers is to create logical gate operations. As discussed above, single-qubit gates correspond to rotations of the (pseudo-)spins. Pulses of RF or MW radiation or laser pulses are a convenient means for implementing such rotations around arbitrary axes. According to eq. (5.18), the rotation axis $\vec{\omega}_{eff}$ can therefore be oriented in any arbitrary direction by adjusting frequency (and thereby $\Delta\omega_L$) and phase φ of the RF field. The angle of rotation $\alpha = \omega_{\text{eff}} \tau_p$ around the effective field, which is called the flip angle, is given by the product of the effective field strength ω_{eff} and the pulse duration τ_p.

Further reading

An excellent reference for the material in this chapter is Chapter 4 of [35] which consists to a large extent of exercises which the reader is encouraged to solve in order to really learn the material. (However, the anticipated results of the exercises are stated clearly enough so that the lazy reader may also get along without solving the exercises.) Preskill [32], Section 6.2.3 discusses universal quantum gates from a different (Lie-group) point of view.

Problems and Exercises

1. Show that the Paul matrices anti-commute, i.e. $\mathbf{XY} + \mathbf{YX} = 0$, and that therefore

$$\left(\frac{2}{\hbar}\vec{n} \cdot \vec{\mathbf{S}}\right)^2 = (n_x \mathbf{X} + n_y \mathbf{Y} + n_z \mathbf{Z})^2 = \mathbf{1},$$

when $\vec{n}$ is a unit vector.